Two- and Three-dimensional Methods for the Assessment of Ballast Mats, Ballast Plates and Other Isolators of Railway Vibration

Lutz Auersch

Federal Institute of Materials Research and Testing (BAM), D 12200 Berlin, Germany

(Received 29 August 2005; accepted 15 September 2006)

This contribution gives a simple two-dimensional method to calculate the dynamics of railway tracks which have been checked against the results of completely three-dimensional finite-element boundary-element calculations. The forces generated by the train are modified, amplified or reduced, by the vehicle-track interaction and the force transfer of the track, yielding the forces that are acting on the ground and exciting the ground-borne vibration. The overall force transfer function, which is the integral of all forces acting on the soil divided by the input force on the vehicle, is presented for a number of different track systems. Details are given for the track with ballast mats where the influence of wheel mass, track mass, subsoil condition, and the stiffness of the mat have been analysed. Experimental results of the Federal Institute of Materials Research and Testing and literature are used to check the theoretical results about ballast mats.

Nomenclature

A – area
A_j – constant
b – width
c_S – soil damping
c' – damping per length
D – material damping
E – modulus of elasticity
EI – bending stiffness
f – frequency
f_{zz} – compliance function
$\boldsymbol{f}$ – compliance matrix
F – force
F_t, F_r, F_z – transversal, radial, vertical force
F_S – total force acting on the soil
F_T – wheel-set force on the track
F_V – exciting force on the vehicle
F'_S, F'_T – force per length
G – shear modulus
h – height
H – total force transfer function F_S/F_V
H_T – track force transfer function F_S/F_T
H_{VT} – vehicle-track force transfer function F_T/F_V
i – imaginary unit
k_S – soil stiffness
K_T – track stiffness
K_V – vehicle stiffness
$\boldsymbol{K}_S$ – soil stiffness matrix
$\boldsymbol{K}_F$ – track stiffness matrix
k' – stiffness per length
k'_S – soil stiffness per length
K'_S – complex soil stiffness $k'_S + i\omega c'_S$
k'_D – dynamic stiffness $k' + i\omega c' - m'\omega^2$
$\boldsymbol{K}'_D$ – dynamic stiffness $\boldsymbol{K}' - \boldsymbol{m}'\omega^2$
k'' – stiffness per area
m_W – wheel-set mass
m' – mass per length
$\boldsymbol{m}'$ – mass matrix of multi-beam track
$\boldsymbol{M}$ – finite element mass matrix
N_{zz} – compliance in wavenumber domain
r – radial distance
s – irregularities of vehicle and track
t – time
u – displacement
u_t, u_r, u_z – transversal, radial, vertical displacement
v_S, v_P – shear and compression wave speed
$\boldsymbol{v}_j$ – eigenvector
x – position along the track
$\boldsymbol{x}$ – position vector
ν – Poisson ratio
ρ – mass density
ξ – wavenumber
ξ_S, ξ_P – shear and compression wavenumber
ω – circular frequency
u'''' – multiple differentiation with respect to x (position)
$\ddot{u}$ – multiple differentiation with respect to t (time)

1. INTRODUCTION

A variety of isolation measures exists to reduce the vibration in the neighbourhood of railway lines. They can be roughly classified as elastic or stiffening systems. The following elastic elements are used (Fig. 1): railpads or resilient fixation systems between rail and sleeper,[1] sleeper shoes under the sleepers,[2] and ballast mats under the ballast[1,3,4]. Stiffening systems (plates) are used as slab tracks,[5-7] floating slab tracks,[1,8,9] or mass-spring systems[10] and in a different way, as an under ballast plate[11-13]. The main interest of this contribution is ballast mats.

Ballast mats are an efficient measure to reduce the vibrations near railway lines. The vehicle-track system gets a low eigenfrequency due to the insertion of an elastic ballast mat under the ballast. For frequencies higher than this low vehicle-track eigenfrequency, the forces, that are generating the vibration of the soil, are considerably reduced.

The reduction of this force F_S acting on the soil is analysed for different tracks – ballasted tracks, non-ballasted tracks, with or without isolation measure – by three-dimensional combined finite element boundary element models or by simple two-dimensional models. The different models are illustrated in Figs. 1 and 2, and the parameters used throughout this paper are listed in the corresponding Tables 1 and 2. The parameters of the two-dimensional model are adjusted so that the two-dimensional results are similar to the three-dimensional results.

Table 1. Parameters of the two-dimensional track model.

wheelset	mass	$m_W/2 = \underline{750}, 1500$ kg
UIC60 rail	flexural stiffness	$EI_R = 6.4 \times 10^6$ Nm^2
	mass per length	$m'_R = 60$ kg/m
rail pads	stiffness	$k_P = 40, 80, 150, \underline{300}$ kN/mm
sleeper	mass	$m_S/2 = 170$ kg
sleeper shoe	stiffness per area	$k''_{SS} = 3 \times 10^8$ N/m^3
ballast	mass density	$\rho_B = 2000$ kg/m^3
	modulus of elasticity	$E^*_B = 0.5, 1.1, \underline{2.2}, 4.4 \times 10^8$ N/m^2
	height	$h_B = 0.35$ m
ballast mat	stiffness per area	$k''_M = 2, \underline{4}, 8, 16 \times 10^7$ N/m^3
concrete plate	modulus of elasticity	$E = 3 \times 10^{10}$ N/m^2
	mass density	$\rho = 2.5 \times 10^3$ kg/m^3
	height	$h_P = 0, 0.25, 0.5, 1$ m
soil	stiffness	$k_S = 2, 4, \underline{8}, 16 \times 10^7$ N/m
	damping	$c_S = 3.8, 5.3, \underline{7.5}, 10.5 \times 10^5$ Ns/m
elastic elements	hysteretic damping	$D = 0.1$
ballast, mat and plate	effective width	$b = 1.3$ m

Table 2. Additional parameters of the three-dimensional track model.

concrete sleepers	modulus of elasticity	$E = 3 \times 10^{10}$ N/m^2
	Poisson's ratio	$\nu = 0.15$
	mass density	$\rho = 2.5 \times 10^3$ kg/m^3
the soil	mass density	$\rho = 2 \times 10^3$ kg/m^3
	Poisson's ratio	$\nu = 0.33$
	shear modulus	$G = 2, 4.5, \underline{8}, 18 \times 10^7$ N/m^2
	shear-wave speed	$v_S = 100, 150, \underline{200}, 300$ m/s
	compression-wave speed	$v_P = 2v_S$
track (ballast, plate)	width	$b_B = b_P = 5.6$ m

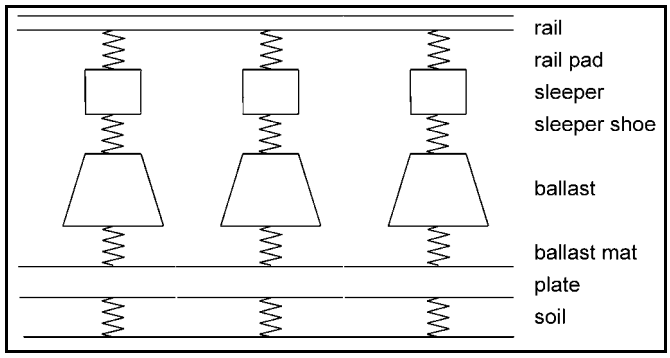

Figure 1. Simple two-dimensional beam-on-support model of the track.

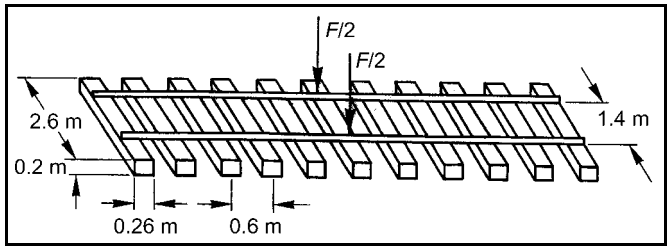

Figure 2. Three-dimensional finite-element boundary-element model of the track.

The 3D calculation of track-soil systems is described in full details in reference[14] for homogeneous soil, whereas the details for layered soils are given in reference[15]. The experimental verification of the 3D method is done by measurements of train, track, and soil vibration.[14]

Similar track-soil models have been established at a number of institutes and have been compared in a benchmark test by the author.[16] There exist more detailed methods[7,13,17] which include infinite tracks and moving load effects. These effects are of interest for very high train speeds and for very soft soils. These methods are also called 2.5D methods[18] as they make use of the homogeneous or periodic structure[19] of the track. On the contrary, much simpler models are used to calculate isolated tracks.[1,3] One problem of the 1D and 2D methods is the choice of the correct parameters. This problem has been solved by fitting the 2D results to the 3D results.

The complete three-dimensional method is described first because it is the base of all calculations (section 2). In section 3, the simple two-dimensional beam-on-support method which is used for most of the results presented here, is given. The different steps of vehicle-track calculation, which are necessary to get the total force transfer function, are explained in section 4 and illustrated by a track with an under-ballast plate. The main part of the contribution (section 5) consists of the calculated force transfer functions of different tracks, especially of tracks with ballast mats. At the end of this section, the force reductions of other railway isolators are presented. Finally, section 6 discusses the practical application of the methods and two experimental examples are given.

2. THREE-DIMENSIONAL FINITE-ELEMENT BOUNDARY-ELEMENT METHOD

A three-dimensional track model is combined with the boundary element formulation of the soil.[20] That means that the Greens' functions of a homogeneous or layered soil[15] are used to establish a fully coupling soil matrix which is added to the FEM matrix of the track.

2.1. Green's Functions of the Soil

The soil is a homogeneous or horizontally layered elastic half-space, which is excited at its surface by dynamic forces F, and the displacements u have to be calculated for surface points, too. The relation between the displacements u and the force F can be described in cylindrical (transversal, radial, and vertical) components as

$$\begin{bmatrix} u_t \\ u_r \\ u_z \end{bmatrix} = \begin{bmatrix} f_{tt} & 0 & 0 \\ 0 & f_{rr} & f_{rz} \\ 0 & -f_{rz} & f_{zz} \end{bmatrix} \begin{bmatrix} F_t \\ F_r \\ F_z \end{bmatrix}. \tag{1}$$

The four functions $f_{ij}(r,\omega)$ can be calculated by integration in wavenumber domain,[15] for example as

$$f_{zz} = \frac{1}{2\pi} \int_0^\infty N_{zz}(\xi) J_0(\xi r) \xi d\xi \tag{2}$$

for the simplest case of the vertical component. J_0 is the Bessel function of the first kind and the vertical compliance N_{zz} in wavenumber domain ξ can be given explicitly for the homogeneous half-space

$$N_{zz} = \frac{\xi_S^2 \sqrt{\xi_P^2 - \xi^2}}{iG\left[(\xi_S^2 - 2\xi^2)^2 + 4\xi^2 \sqrt{\xi_S^2 - \xi^2}\, \sqrt{\xi_P^2 - \xi^2} \right]}, \tag{3}$$

with the abbreviations

$$\xi_S = \omega / v_S; \quad \xi_P = \omega / v_P, \tag{4}$$

or calculated by matrix methods for a layered soil.[15] Similar formulas hold for the other components and the complete set of Green's functions Eq. (1) is used in the present boundary element method of the soil.

2.2. The Stiffness Matrix of the Discretised Soil

First, the soil has to be defined by a set of m surface points with coordinates $\boldsymbol{x}_\alpha$. A certain portion A_α of the surface area belongs to each surface point. A force $\boldsymbol{F}$ at a point $\boldsymbol{x}_\alpha$ of the surface of the soil is considered. By using the Green's functions (of the preceding section), the displacements at all other points $\boldsymbol{x}_\beta$ are calculated

$$\begin{bmatrix} u_x \\ u_y \\ u_z \end{bmatrix} = \begin{bmatrix} f_{rr} x_r^2 + f_{tt} y_r^2 & (f_{rr} - f_{tt}) x_r y_r & f_{rz} x_r \\ (f_{rr} - f_{tt}) x_r y_r & f_{rr} y_r^2 + f_{tt} x_r^2 & f_{rz} y_r \\ -f_{rz} x_r & -f_{rz} y_r & f_{zz} \end{bmatrix} \begin{bmatrix} F_x \\ F_y \\ F_z \end{bmatrix}, \tag{5}$$

with

$$x_r = (x_\beta - x_\alpha)/r; \quad y_r = (y_\beta - y_\alpha)/r.$$

Equation (5) is the same as Eq. (1), but transformed into the cartesian coordinate system.

For the point of excitation $\boldsymbol{x}_\alpha$ itself, the Green's function cannot be evaluated because the solution is singular at this point. This difficulty can be overcome by calculating the mean value over the corresponding surface area. This leads to the mean values of the scalar functions $f_{ii}(r)$

$$\bar{f}_{ii} = \frac{2}{r_\alpha^2} \int_0^{r_\alpha} f_{ii}(r) r dr, \tag{6}$$

where r_α is the radius of area A_α. So the compliance relation at the excited point of the soil is

$$\begin{bmatrix} u_x \\ u_y \\ u_z \end{bmatrix} = \begin{bmatrix} \frac{\bar{f}_{rr} + \bar{f}_{tt}}{2} & 0 & 0 \\ 0 & \frac{\bar{f}_{rr} + \bar{f}_{tt}}{2} & 0 \\ 0 & 0 & \bar{f}_{zz} \end{bmatrix} \begin{bmatrix} F_x \\ F_y \\ F_z \end{bmatrix}. \tag{7}$$

The flexibility matrix of the soil is assembled of all these 3×3 matrices $\boldsymbol{f}_{\beta\alpha}$

$$\begin{bmatrix} \boldsymbol{u}_1 \\ \vdots \\ \boldsymbol{u}_\beta \\ \vdots \\ \boldsymbol{u}_m \end{bmatrix} = \begin{bmatrix} \boldsymbol{f}_{11} & \cdots & \boldsymbol{f}_{1\alpha} & \cdots & \boldsymbol{f}_{1m} \\ \vdots & \ddots & \vdots & \ddots & \vdots \\ \boldsymbol{f}_{\beta 1} & \cdots & \boldsymbol{f}_{\beta\alpha} & \cdots & \boldsymbol{f}_{\beta m} \\ \vdots & \ddots & \vdots & \ddots & \vdots \\ \boldsymbol{f}_{m1} & \cdots & \boldsymbol{f}_{m\alpha} & \cdots & \boldsymbol{f}_{mm} \end{bmatrix} \begin{bmatrix} \boldsymbol{F}_1 \\ \vdots \\ \boldsymbol{F}_\alpha \\ \vdots \\ \boldsymbol{F}_m \end{bmatrix}, \tag{8a}$$

with m the number of points, or in short form

$$\boldsymbol{u} = \boldsymbol{f}\boldsymbol{F}. \tag{8b}$$

The inversion of this equation

$$\boldsymbol{F} = \boldsymbol{f}^{-1}\boldsymbol{u} =: \boldsymbol{K}_S \boldsymbol{u} \tag{9}$$

gives the dynamic stiffness matrix $\boldsymbol{K}_S = \boldsymbol{f}^{-1}$ of the soil which is introduced in the finite element procedure for the structure.

2.3. Combined Finite-Element Boundary-Element Method

Now the coupling of both subsystems, track and soil, is done by introducing the soil into the finite element code as a new type of element. The points of the soil define one special element of which the dynamic stiffness matrix $\boldsymbol{K}_S$ is calculated by the boundary element method. The track structure is described by the conventional finite-element method. Local stiffness matrices, as well as local mass matrices, are assembled in a global stiffness matrix, $\boldsymbol{K}_0$, and a global mass matrix $\boldsymbol{M}$, respectively. Combining these matrices, the frequency-dependent dynamic stiffness matrix $\boldsymbol{K}_F(\omega)$ of the track structure

$$\boldsymbol{K}_F = \boldsymbol{K}_0 - \omega^2 \boldsymbol{M} \tag{10}$$

is obtained. Then, the coupling of the boundary-element and finite element part of the system can be expressed in terms of global representations of the matrices and

$$\boldsymbol{F} = (\boldsymbol{K}_F(\omega) + \boldsymbol{K}_S(\omega))\,\boldsymbol{u} \tag{11}$$

is the equation of the whole track-soil system. This has to be solved for given external forces $\boldsymbol{F}$, for example the wheel-set forces of Fig. 2.

From the solution of Eq. (11), the stiffness, K_T, of the track under the wheel-set load and the force transfer function, H_T,

of the track are calculated, which relate the displacement, u_T, of the rail under the wheel and the (complex) sum of the soil forces, F_S, below the track to the exciting wheel-set load F_T. These FEBEM results are used for further vehicle-track analyses.

In this contribution, the finite-element model of the track consists of two rails and eleven sleepers (Fig. 1). The rails are represented by 2×40 Euler beam elements, the sleepers by 11×12 plate elements. The ballast is modelled by $44\times 48\times 3$ eight-node solid elements. An underlying plate consists of 44×48 plate elements. The elastic elements are modelled as 2×11 truss elements (railpads) or as 44×48 solid elements (ballast mat). The parameters used in this contribution are given in Tables 1 and 2. The parameters of the elastic elements are in the range of available products. Only one type of elastic element is applied at a time. The underlined values are used as standard if the corresponding parameter is not varied.

3. SIMPLE TWO-DIMENSIONAL BEAM-ON-SUPPORT METHOD

The track model consists of a rail beam which is supported on a combination of spring, damper, and mass elements (Fig. 1). These elements represent railpads, sleepers, the ballast, and any isolation measure. The assembly of all these elements can be represented by a dynamic, frequency-dependent support stiffness per length k'_D. The most simple model would be a mass m' on a spring k' and a damper c'

$$k'_D = k' + c'i\omega - m'\omega^2. \tag{12}$$

The stiffness of such a beam-on-support track system is derived as follows:

A beam on continuous support is described by the differential equation

$$EI\,u'''' + k'u + c'\dot{u} + m'\,\ddot{u} = 0 \tag{13}$$

for the displacement u. If the complex exponential function

$$u = Ae^{(\xi x + i\omega t)} \tag{14}$$

is inserted into the differential equation, the following condition for the wavenumber ξ is obtained

$$EI\xi^4 + k' + c'i\omega - m'\omega^2 = 0. \tag{15}$$

This equation has four roots

$$\xi_{1,2,3,4} = \left(-\frac{k' + c'i\omega - m'\omega^2}{EI}\right)^{1/4} \tag{16}$$

of which the both wavenumbers with negative real part are chosen so that the solution is decreasing in x-direction

$$\xi_1 = \xi_0\frac{-1+i}{\sqrt{2}}; \quad \xi_2 = \xi_0\frac{-1-i}{\sqrt{2}},$$

with ξ_0 the principal value of the root

$$\xi_0 = \left(\frac{k' + c'i\omega - m'\omega^2}{EI}\right)^{1/4}.$$

The solution is found by fitting the general solution Eq. (14) to the boundary conditions as

$$u(x=0) = \frac{\xi_2 - \xi_1}{\xi_2}A;\; F = 2EI\,u'''(x=0) = 2EI\frac{\xi_2\xi_1^3 - \xi_1\xi_2^3}{\xi_2}A.$$

Therefore, the stiffness of the track can be expressed as

$$K_T = \frac{F}{u} = \frac{2EIu'''}{u} = 2EI\frac{\xi_2\xi_1^3 - \xi_1\xi_2^3}{\xi_2 - \xi_1}$$

$$= -2EI\xi_1\xi_2(\xi_1 + \xi_2) = 2EI\xi_0^3\sqrt{2};$$

$$K_T = 2\sqrt{2}\,EI^{1/4}(k' + c'i\omega - m'\omega^2)^{3/4}. \tag{17}$$

The transfer function H_T of the force is the ratio of the force F_S acting on the soil to the wheel load F_T acting on top of the track. It can be calculated for a single support chain if the mass of the rail is included. This remarkable result, which further simplifies the force transfer function of the track, is proved in the appendix. For the simple support model it follows

$$H_T = \frac{F_S}{F_T} = \frac{F'_S}{F'_T} = \frac{k' + c'i\omega}{k' + c'i\omega - m'\omega^2}. \tag{18}$$

Equations (17) and (18) are the simplest versions for a beam-on-support system. The support can be more complex and be calculated with transfer matrices.[21] A general method for the combination of support elements with more than one beam is given in the appendix.

Although the method is simple, it is not easy to get appropriate parameters for the model. The simple two-dimensional models have been calibrated by the FEBEM results. Rules for the parameters of the simple model are established by approximating the dynamic FEBEM-stiffness of the track.[21,22] The results of the simple method presented in this paper are quite similar to corresponding results of the three-dimensional finite-element boundary-element method. Namely, the vehicle-track eigenfrequencies are the same for both methods if the parameters of the simple model are properly chosen.

4. VEHICLE-TRACK INTERACTION

The track model is combined with a vehicle model. A single rigid wheel mass m_W is used throughout this paper. The dynamic stiffness $K_V = -m_W\omega^2$ of the vehicle is introduced into the vehicle-track-interaction analysis. A force F_V acting on the vehicle yields a force F_T acting on the track according to

$$H_{VT} = \frac{F_T}{F_V} = \frac{K_T}{K_T + K_V}, \tag{19}$$

and a force F_S on the soil according to

$$H = \frac{F_S}{F_V} = \frac{F_S}{F_T}\frac{F_T}{F_V} = \frac{F_S}{F_T}\frac{K_T}{K_T + K_V} = H_T H_{VT}. \tag{20}$$

For the simplest two-dimensional case, the result can be given explicitly as

$$\frac{F_S}{F_V} = \frac{k' + i\omega c'}{k' + i\omega c' - m'^*\omega^2}, \tag{21}$$

which looks almost as simple as a single-degree-of-freedom oscillator. However, m'^* is a frequency-dependent combination of the wheel and track mass.

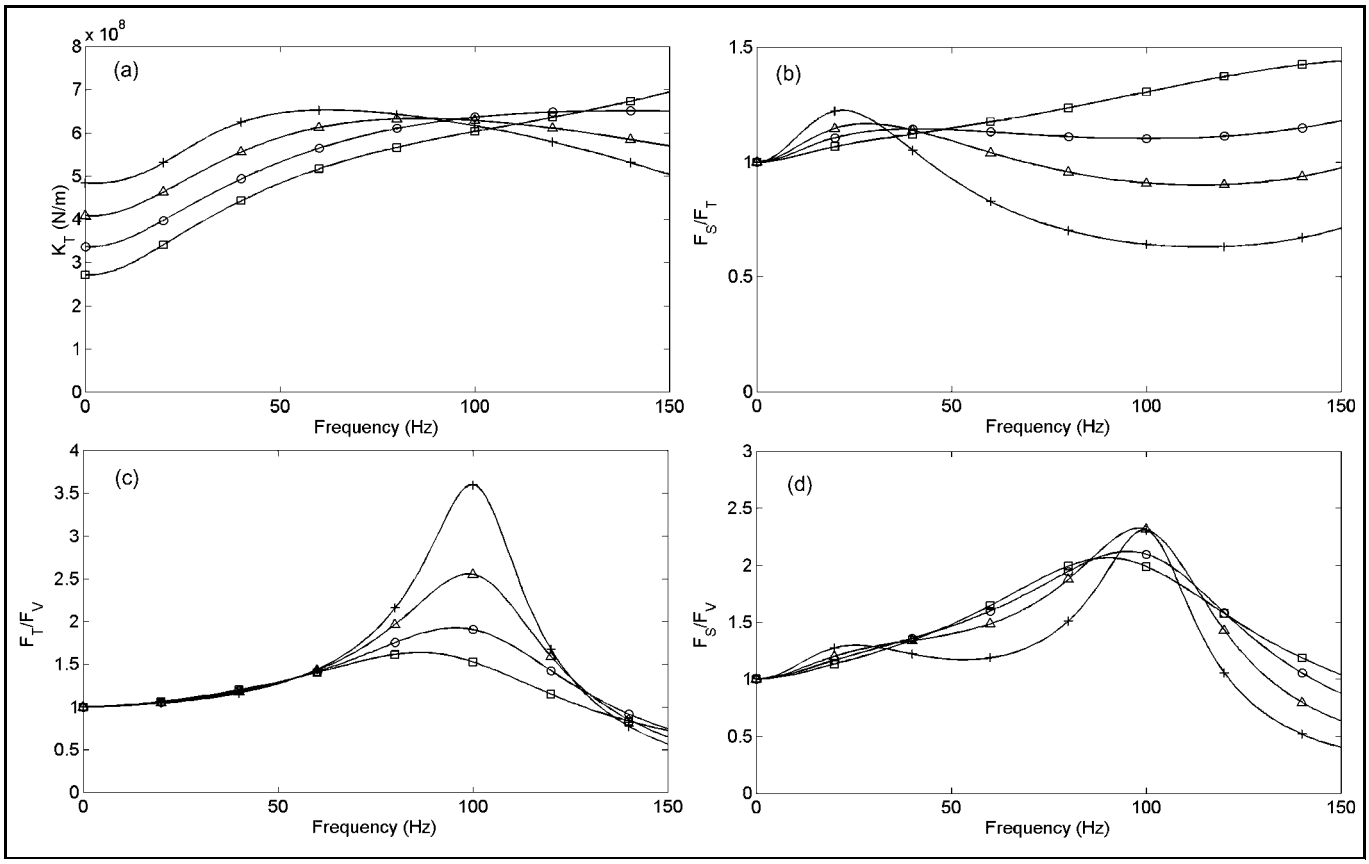

Figure 3. 2D ballasted track on a concrete plate of $h_P = 0(\square), 0.25(\mathrm{O}), 0.5(\triangle), 1(+)$ m, (a) stiffness K_T and (b) force transfer H_T of the track, (c) vehicle-track transfer function H_{VT}, (d) and total force transfer function H.

The four steps of calculation with their results K_T, H_T, H_{VT}, and H are illustrated by Fig. 3 for ballasted tracks on different plates (2D models). The static stiffness of the track increases with increasing height of the plate (Fig. 3(a)), but the situation changes at high frequencies. The force transfer of the track (Fig. 3(b)) shows a moderate resonance at low frequencies which is a resonance of the heavy ballast-plate track on the soil. A corresponding force reduction is found around 100 Hz, especially for the thickest plate. The vehicle-track interaction (Fig. 3(c)) yields another more pronounced resonance at 100 Hz which is mainly ruled by the wheel-set mass and the ballast stiffness. The height of the plate has only a slight influence on the resonance frequency, but the resonance amplitude is increased for thicker plates. The overall force transfer (Fig. 3(d)), which is the product of the force transfer of the track and the vehicle track interaction, displays both resonance frequencies. Only minor reductions of the force can be found in the given frequency range.

5. FORCE TRANSFER OF DIFFERENT TRACKS

The two- and three-dimensional methods have been used to calculate a number of different tracks with and without isolation measures. For each track, the specific parameters, which are important for the force transfer from the vehicle to the soil, have been investigated.

5.1. Conventional Tracks

A ballasted track on a homogeneous subsoil is highly influenced by the stiffness of this subsoil (Fig. 4). The vehicle-track eigenfrequency can vary between 50 Hz and more than

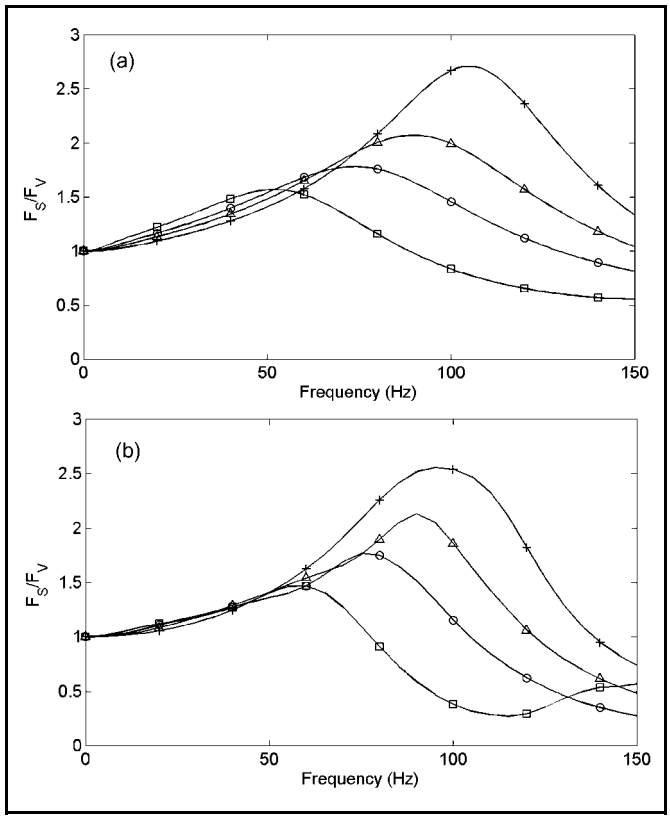

Figure 4. Track on homogeneous subsoil (a) 2D results with $k'_S = 2(\square), 4(\mathrm{O}), 8(\triangle), 16(+) \times 10^7$ N/m^2 and $c'_S = 3.8(\square), 5.3(\mathrm{O}), 7.5(\triangle), 10.5(+) \times 10^5$ Ns/m^2, (b) 3D results with shear wave speeds $100(\square), 150(\mathrm{O}), 200(\triangle), 300(+)$ m/s.

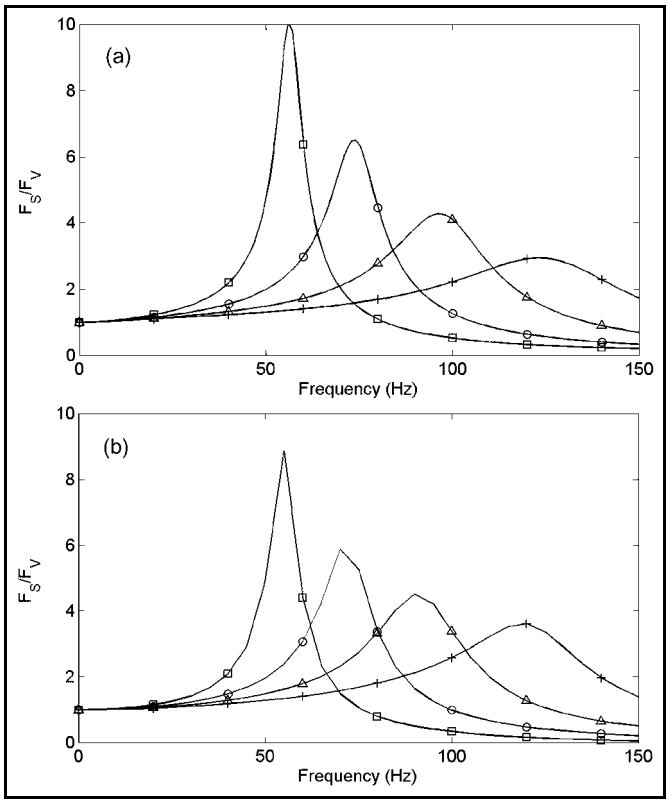

Figure 5. Slab track with different railpads $k_P = 40(\square), 80(\mathrm{O}), 160(\triangle)$, 300(+) kN/mm, (a) 2D results, (b) 3D results.

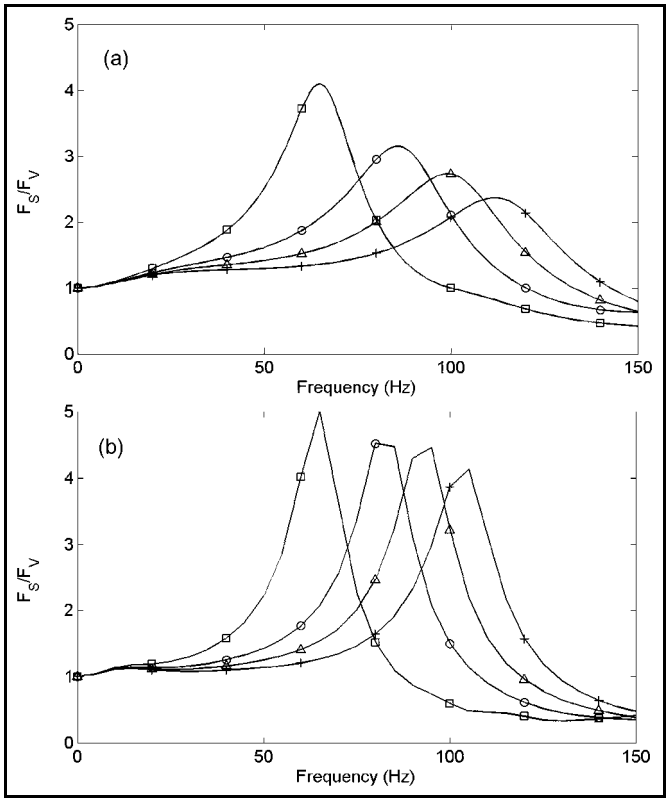

Figure 6. Ballast track on a plate of $h_P = 0.5$ m, ballast stiffness $E_B^* = 0.5(\square), 1.1(\mathrm{O}), 2.2(\triangle), 4.4(+) \times 10^7$ N/m^2, (a) 2D results, (b) 3D results.

100 Hz (for wheel-sets of 1500 kg). The resonance is highly damped by the radiation in the soil. There is a reduction of the force at frequencies higher than the resonance frequency, but this is a minor effect for conventional tracks and the frequency range of interest. Figure 5 shows results for slab tracks where the sleepers are placed on a concrete plate ($h_P = 0.2$ m) instead of the ballast. Slab tracks are usually constructed with elastic railpads which determine the stiffness of the track and the vehicle-track resonance. Elastic railpads can provide the same compliance that ballasted tracks have and yield similar eigenfrequencies. The resonance amplitudes, however, are considerably higher as the radiation damping is impeded (there is no material damping for this example). If the ballasted track is laid on a plate, for example the tunnel floor, the most important parameter is the stiffness of the ballast (Fig. 6). The vehicle-track eigenfrequency is a little higher and the damping is reduced compared to a track on a soil with corresponding stiffness (see Fig. 4).

5.2. Ballast Mat Tracks

A ballast mat supports the ballast mass in addition to the sleeper, rail, and wheel masses. Therefore, eigenfrequencies as low as 20 Hz are possible, depending on the stiffness of the mat (Fig. 7). For higher frequencies, the force amplitudes are strongly reduced where the strongest reduction is obtained for the softest mat and the lowest eigenfrequency. A number of calculations – 2D as well as 3D – have shown the following effects. The wheel mass has only a minor influence (Fig. 8). For wheel-set masses between 1000 and 3000 kg, the shift of the resonance frequency is only 20%, which demonstrates that the track mass and especially the ballast mass is of importance. The subsoil has almost no influence on the performance of the ballast mat (Fig. 9). A soft soil increases the damping. A stiff soil, as well as a plate under the ballast mat, cannot improve the effect of a ballast mat, but they can reduce the damping.

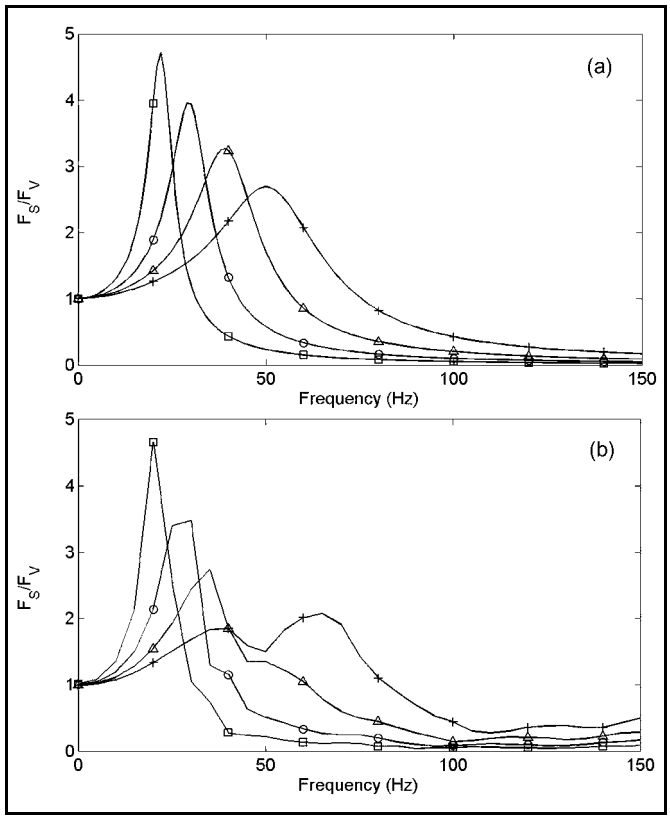

Figure 7. Track on a ballast mat of stiffness $k_M'' = 2(\square), 4(\mathrm{O}), 8(\triangle), 16(+) \times 10^7$ N/m^3, (a) 2D results, (b) 3D results.

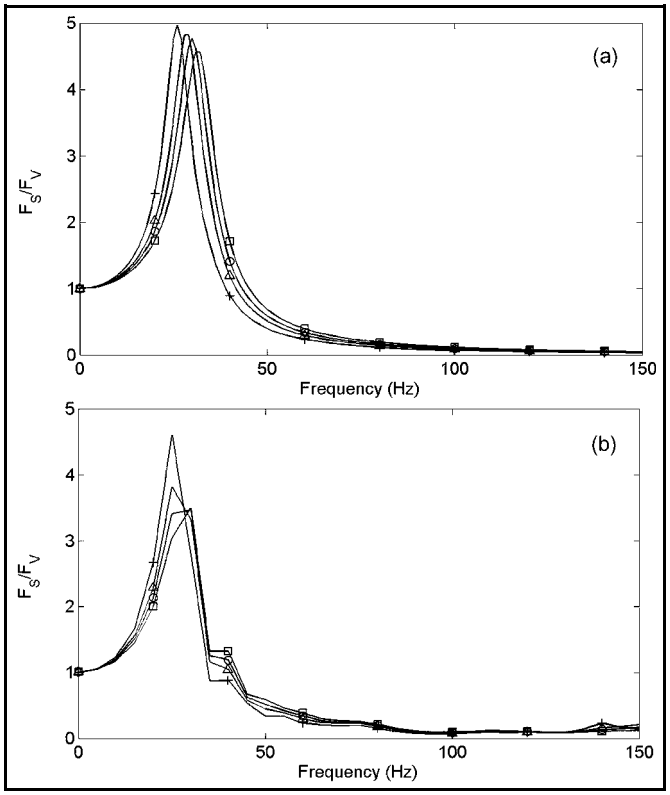

Figure 8. Track on a ballast mat with different wheel-set mass $m_W = 1000(\square), 1500(\mathrm{O}), 2000(\triangle), 3000(+)$ kg, (a) 2D results, (b) 3D results.

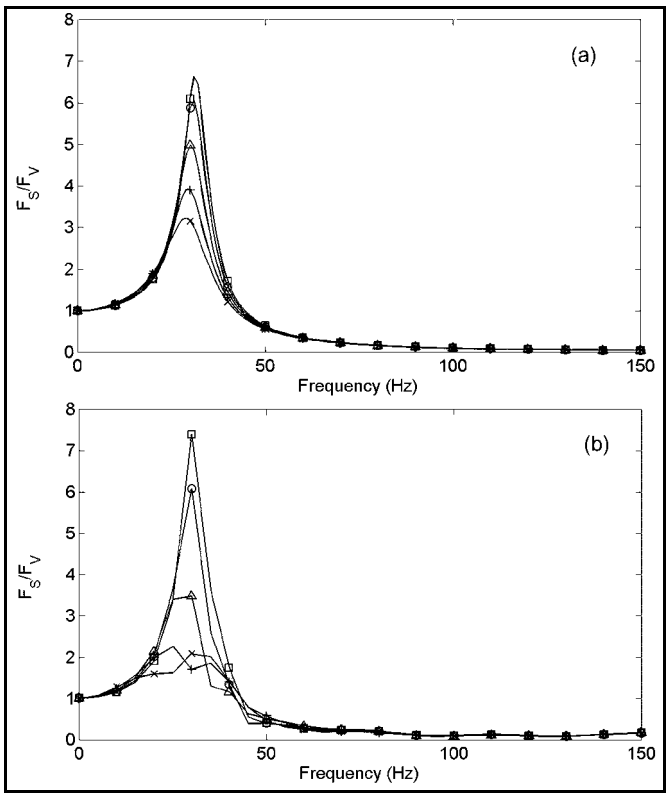

Figure 9. Tracks on a ballast mat on different soils, shear wave speed $v_S = 1000(\square), 500(\mathrm{O}), 300(\triangle), 200(+), 150(\times)$ m/s, (a) 2D results, (b) 3D results.

5.3. Other Isolators of Railway Vibration

Figure 10 gives an overview of the results of different tracks. A conventional track is compared with tracks on isolators. The isolators are elastic elements placed at different places of the track. The lower the position of the isolator, the greater the supported mass. The lower the eigenfrequency of the system and the better the obtained reduction of the force. While the conventional track has a resonance at 90 Hz (Fig. 10 □), it is shifted to 70 Hz for the track with medium soft railpads (Fig. 10 O). If there is a ballast track with sleeper shoes, more mass is elastically supported and a lower vehicle-track eigenfrequency is achieved at 50 Hz (Fig. 10 △). Ballast mat tracks further reduce the eigenfrequency to 30 Hz (Fig. 10 +). Floating slab tracks which are using the same mats would result in approximately the same eigenfrequencies as mats under ballast tracks. In Fig. 10, a lower tuning frequency of the floating slab track (light weight mass-spring system) is assumed. Heavy mass-spring systems resting on an elastic strip or on single elements can have very low eigenfrequencies (Fig. 10 ◇). According to that, they have the highest reduction of the forces and ground-borne vibrations.

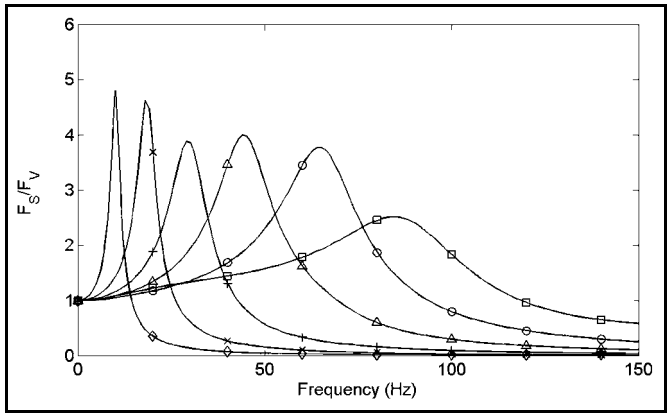

Figure 10. Tracks with different isolation measures, □ ballast track on a plate, O slab track with elastic rail pads ($k_P = 60$ kN/mm), △ ballast track with sleeper shoes ($k''_{SS} = 12\times10^7$ N/m^3), + ballast track with ballast mat ($k''_M = 4\times10^7$ N/m^3),× floating slab track and ◇ heavy mass-spring system, 2D results.

5.4. Comparison of 2D and 3D Results

The 2D and 3D results are given together in Figs. 4 through 9. The general agreement is very good, especially regarding that the 2D parameters are chosen by a general rule and not by fitting each curve. Of course, there are more details in the 3D results, for example two maxima instead of one in Fig. 7(a), curve + and Fig. 9(a), curve × and +, and a related frequency shift. This might be due to bending of the sleepers and waves in the ballast. (The minimum between the two maxima is at the frequency where the shear wavelength equals the ballast width.) But these differences between 2D and 3D results are not so significant. The 2D method is much faster and yields acceptable results so that it is more convenient for a railway design engineer.

6. EXPERIMENTAL RESULTS

The isolation effect of the different track systems has to be checked experimentally. For the under-ballast mat, two practical examples are presented. The first example is a ballast mat with stiffness $k''_M = 4\times10^7$ N/m^3, which is installed in a surface line on a soft soil (modelled as $v_S = 100$ m/s, all other parameters are chosen as the standard values of this contribution).

Figure 11(a) shows the corresponding two force transfer functions. They have a resonance at $f = 30$ Hz with mat and at $f = 55$ Hz without mat. The ratio of these transfer functions is

$$\frac{F_S}{F_V}_{\text{with mat}} \Big/ \frac{F_S}{F_V}_{\text{without mat}},$$

and yields the relative force amplitude (Fig. 11(b)). Due to the small difference between these two resonance frequencies, the reduction at high frequencies is limited to 1:3 to 1:4 (−10 to −12 dB). The vibration amplitudes have been measured at two neighboured track sections, one section with a ballast mat, one section without a ballast mat. The relative vibration amplitudes of these two sections are shown in Fig. 11(b). The measured vibration reduction is a little worse than the theoretical force reduction, but in general, the theoretical and experimental curve agree well. Similar experimental results for ballast mats in surface lines are reported in Nelson.[1] The agreement of force and vibration reduction may be expected because the total force acting on the soil is the only source of the soil vibration if the measuring point is far enough away from the quasi static-track deformation.

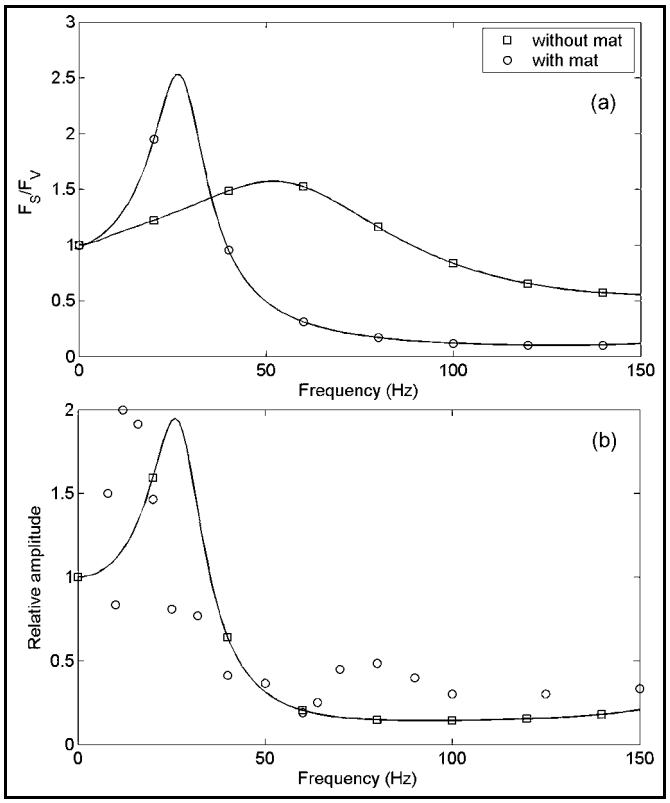

Figure 11. Track on soft soil with and without ballast mat, (a) force transfer functions, (b) □ relative force amplitudes (theory) and O relative vibration amplitudes (measurement).

The second example is a track in a tunnel for which the isolation effect is demonstrated in Fig. 12. The soil and ballast are modelled with $v_S = 200$ m/s. The stiffness of the ballast mat is $k''_M = 4 \times 10^7$ N/m^3, and the unsprung mass of the vehicle is $m_W = 3000$ kg, according to Wettschureck.[3] The tunnel base plate reduces the radiation damping of the soil, and the resonances at $f = 25$ and 70 Hz are more pronounced (Fig. 12(a)). The reduction at high frequencies reaches values of 1:10 (–20 dB). The theoretical and experimental reduction agree very well, demonstrating the high performance of ballast-mat tracks in case of a tunnel line.

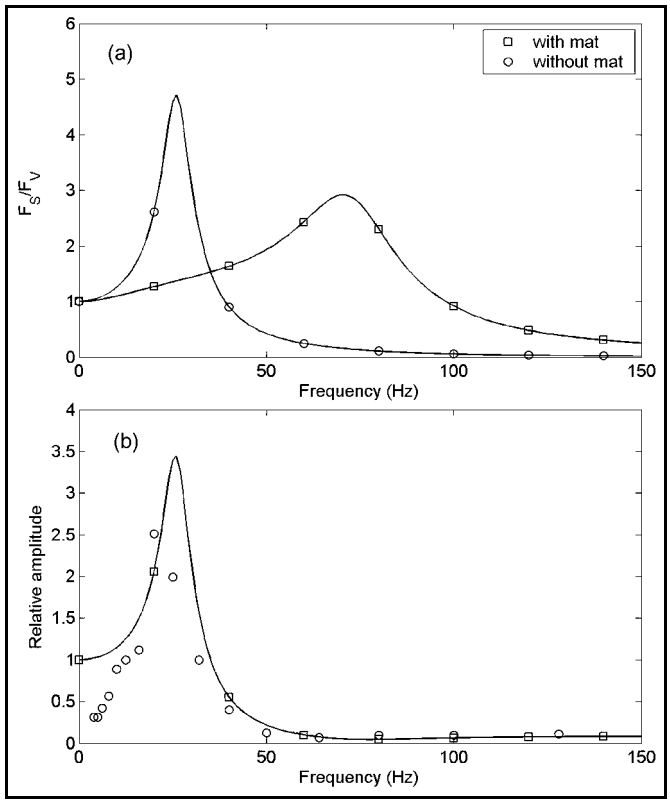

Figure 12. Tunnel track with and without ballast mat, (a) force transfer functions, (b) □ relative force amplitudes (theory) and O relative vibration amplitudes (measurement).

There is a principal error found in the measured reduction curve. From the measurement, it might be concluded that there is a significant reduction at low frequencies $f < 10$ Hz. Actually, this is a systematic error which occurs if the vibration amplitudes are measured at or close to the track. At these measuring points, the low frequency passage of the static train loads are included in the measured signals. The wider load distribution along the track leads to a reduced response to these passing static loads. But this effect will not be found at far-field points.[23] Therefore, measuring points at a longer distance from the track should be preferred to get a realistic vibration reduction.

Besides the modified load distribution, there is another non-dynamic effect of isolating track systems. Elastic, as well as stiffening elements, may have an influence on the track stability. A ballast mat may cause more ballast settlements due to stronger ballast vibration. In a tunnel track or for surface tracks with under-ballast mat and plate,[24] the side walls prevent this track detoriation. Plate tracks have a better track quality which yields lower vibration amplitudes at low frequencies. This has been found more or less pronounced in several measurements.[5,6,25] Under-ballast plates (without mats) show a similar reduction at low frequencies.[25]

The methods presented in this contribution are suited to predict the effectiveness of isolation measures realistically. Moreover, they are used to perform complete predictions for a vehicle-track-soil-building situation.[21,26] The force transfer function is used to calculate the resulting soil force, F_S, for vehicle forces, F_V, or for the main source of train induced vibration, the irregularities, s, of the vehicle and the track[6] which are introduced into the calculation as $F^*_V = K_V s$. In a second and third step, the vibration amplitudes of the soil and

nearby buildings are calculated where the effect of the load distribution of F_S is introduced in an approximate manner.[6] Such a validated simple tool for the force transfer of tracks, the isolation performance and the prediction of environmental vibration will be useful for railway operators and permanent way designers.

7. CONCLUSIONS

Two methods are available to calculate tracks with isolation measures, the three-dimensional finite-element boundary-element method and the simple two-dimensional beam-on-support method. Results are presented about railway tracks without and with ballast mats. The reduction of the forces acting on the ground is considerable. The influence of a number of parameters is analysed. The most important parameters are the mat stiffness, the track mass, and, partly, the wheel mass. The methods have also been applied to other isolation measures at railway tracks such as soft railpads, elastic sleeper shoes, lightweight floating slab tracks, and heavy mass-spring systems. It turns out that each system has a specific frequency range. The system with the lowest vehicle-track eigenfrequency yields the best reduction but this may be the most expensive reduction measure. Therefore, the best reduction measure must be chosen according to the situation at hand.

APPENDIX. TWO-DIMENSIONAL MULTI-BEAM METHOD

The track system consists of n beams with bending stiffness EI_i and mass density m_i'. Between the beams, there are support elements as springs, dampers, masses, and columns. The multi-beam system is described by a set of n differential equations

$$\boldsymbol{EI}\,\boldsymbol{u}'''' + \boldsymbol{m}'\,\ddot{\boldsymbol{u}} + \boldsymbol{K}'\boldsymbol{u} = \boldsymbol{0}, \tag{A1}$$

and a set of boundary conditions

$$\boldsymbol{EI}\,\boldsymbol{u}'''(0) = \frac{F}{2}\boldsymbol{e}_1\,; \quad \boldsymbol{u}'(0) = \boldsymbol{0}, \tag{A2}$$

$\boldsymbol{EI}$ is a diagonal matrix of the EI_i, and $\boldsymbol{m}'$ is a diagonal matrix of the m_i', and $\boldsymbol{K}'$ is a $n\times n$ matrix assembled from the 2×2 dynamic stiffness matrices $\boldsymbol{K}_{ij}$ of each support section. The solution for this track system – for one of the symmetric halves of the system – is found as

$$\boldsymbol{u}(x) = \sum_{j=1}^{2n} A_j \boldsymbol{v}_j e^{\xi_j x}, \tag{A3}$$

with the solutions ξ_i of the eigenvalue problem

$$(\boldsymbol{EI}\xi^4 - \boldsymbol{m}'\omega^2 + \boldsymbol{K}')\boldsymbol{u} = \boldsymbol{0}\,;$$

$$\boldsymbol{EI}^{-1}(\boldsymbol{m}'\omega^2 - \boldsymbol{K}')\boldsymbol{u} = \xi^4\boldsymbol{I}\,; \quad \boldsymbol{A}u = \lambda\boldsymbol{I}, \tag{A4}$$

with the corresponding eigenvectors $\boldsymbol{v}_j$. The $2\times n$ eigenvalues with a negative real part are chosen from the $4\times n$ roots of the n eigenvalues ξ^4 in order to get the physically correct solution for positive values of x. The contribution, A_j, of each eigenform, $\boldsymbol{v}_j$, is calculated from the system of $2\times n$ linear boundary conditions

$$\boldsymbol{u}'(0) = \sum_{j=1}^{2n} \boldsymbol{v}_j \xi_j A_j = 0\,;\ \boldsymbol{u}'''(0) = \sum_{j=1}^{2n} \boldsymbol{v}_j \xi_j^3 A_j = \frac{F}{2}\boldsymbol{EI}^{-1}\boldsymbol{e}_1\,. \tag{A5}$$

The solution Eq. (A3) gives the compliance or stiffness of the track as $N_T = 1/K_T = u_1(0)$ and the force on the soil is calculated as

$$F_S = \int_{-\infty}^{\infty} K_S' u_n(x)\,dx = 2K_S' \int_0^{\infty} \sum_{j=1}^{2n} A_j v_{jn} e^{\xi_j x} dx$$

$$= 2K_S' \sum_{j=1}^{2n} A_j v_{jn} \int_0^{\infty} e^{\xi_j x} dx = 2K_S' \sum_{j=1}^{2n} \frac{A_j v_{jn}}{\xi_j}. \tag{A6}$$

There is another way to calculate the force transfer of the track. The following relations hold for the integrals of the forces and displacements

$$\int_{-\infty}^{\infty} \boldsymbol{F}'\,dx = (\boldsymbol{K}' - \boldsymbol{m}'\omega^2) \int_{-\infty}^{\infty} \boldsymbol{u}\,dx = \boldsymbol{K}_D' \int_{-\infty}^{\infty} \boldsymbol{u}\,dx\,;$$

$$\int_{-\infty}^{\infty} \boldsymbol{u}\,dx = \boldsymbol{K}_D'^{-1} \int_{-\infty}^{\infty} \boldsymbol{F}'\,dx\,, \tag{A7}$$

because the bending stiffness redistributes the load without modifying the total force. Therefore, the total force F_S can be given as

$$F_S = \int_{-\infty}^{\infty} F_S' dx = K_S' \int_{-\infty}^{\infty} u_n dx = K_S'(K_D'^{-1})_{n1} \int_{-\infty}^{\infty} F_T' dx$$

$$= K_S'(K_D'^{-1})_{n1} F_T\,. \tag{A8}$$

The force transfer of the track is determined by the dynamic stiffness, K', of the support elements and the mass, $\boldsymbol{m}'$, of the beams, whereas the bending stiffness has no influence.[27]

Equation (A8) reads as

$$F_S = K_S'(K_D'^{-1})_{n1} F_T = \frac{k' + c'i\omega}{k' + c'i\omega - m'\omega^2} F_T\,, \tag{A9}$$

for a single rail beam and a simple support and this proves Eq. (18) of section 3.

REFERENCES

1. Nelson, J. Recent developments in ground-borne noise and vibration control, *Journal of Sound and Vibration*, **193**, 367-376, (1996).
2. Muller-Boruttau, F. and Kleinert, U. Innovative ballasted track – concrete sleepers with sole pads, World Congress on Railway Research, Cologne, CD-ROM, (2001).
3. Wettschureck, R. and Kurze, U. Einfügungsdämmaß von Unterschottermatten, *Acustica*, **58**, 177-182, (1985).
4. Hanson, C. and Singleton, H. Performance of ballast mats on passenger railroads: Measurement vs. projections, *Journal of Sound and Vibration*, **293**, 873-877, (2006).
5. Auersch, L. The influence of the track on railway induced ground vibration, Proc. 30. Deutsche Jahrestagung fur Akustik (DAGA)/ 7 Congres Francais d'Acoustique (CFA), Strasbourg, 1079-1080, (2004).
6. Auersch, L. The excitation of ground vibration by rail traffic: Theory of vehicle-track-soil interaction and measurements on high-speed lines, *Journal of Sound and Vibration*, **284**, 103-132, (2005).

[7] Sheng, X., Jones, C., and Thompson, D. A theoretical model for ground vibration from trains generated by vertical track irregularities, *Journal of Sound and Vibration*, **272**, 937-965, (2004).

[8] Hussein, M. and Hunt, H. An insertion loss model for evaluating the performance of floating-slab track for underground railway tunnels, Proc. 10th ICSV, Stockholm, (2003).

[9] Lombaert, G. and Degrande, G. The isolation of railway induced vibrations by means of resilient track elements, Proc. 6th Int. Conf. on Structural Dynamics (Eurodyn 2005), Millpress, Rotterdam, 645-650, (2005).

[10] Müller, G., Diehl, R., and Dörle, M. Assessment of the insertion loss of mass spring systems for railway lines and methods for the prediction of noise and vibration quantities, Proc. Euro Noise, Munchen, 97-102, (1998).

[11] Jones, C. Use of numerical models to determine the effectiveness of anti-vibration system for railways, Proc. Instn Civ. Engrs Transp., 43-51, (1994).

[12] Kaynia, A., Madshus, C., and Zackrisson, P. Ground vibration from high-speed trains: Prediction and countermeasure, *J. of Geotechnical and Geoenvironmental Engineering*, **126**, 531-537, (2000).

[13] Takemiya, H. Controlling track-ground vibration due to highspeed train by WIB, Proc. 6th Int. Conf. on Structural Dynamics (Eurodyn 2002), Swets & Zeitlinger, Lisse, 497-502, (2002).

[14] Auersch, L. Dynamics of the railway track and the underlying soil: the boundary-element solution, theoretical results and their experimental verification, *Vehicle System Dynamics*, **43**, 671-695, (2005).

[15] Auersch, L. Wave propagation in layered soil: theoretical solution in wavenumber domain and experimental results of hammer and railway traffic excitation, *Journal of Sound and Vibration*, **173**, 233-264, (1994).

[16] Rücker, W., Auersch, L., Baeßler, M., Knothe, K., Wu, Y., Gerstberger, U., Popp, K., Kruse, H., Savidis, S., Hirschauer, R., Bode, C., Schepers, W., Schmid, G., and Friedrich, K. A comparative study of results from numerical track-subsoil calculations, *System Dynamics and Long-Term Behaviour of Railway Vehicles, Track and Subgrade*, Springer, Berlin, 471-488, (2003).

[17] Aubry, D., Clouteau, D., and Bonnet, G. Modelling of wave propagation due to fixed or mobile dynamic sources, *Wave Propagation and Reduction of Vibrations* (*Wave 1994*), Berg-Verlag, Bochum, 109-121, (1994).

[18] Jean, P., Guigou, C., and Villot, M. A 2.5D BEM model for ground structure interaction, *Building Acoustics*, **11**, 1-17, (2004).

[19] Degrande, G., Clouteau, D., Othman, R., Arnst, M., Chebli, H., Klein, R., Chatterjee, P., and Janssens, B. A numerical model for ground-borne vibrations from underground railway traffic based on a periodic finite element–boundary element formulation, *Journal of Sound and Vibration*, **293**, 645-666, (2006).

[20] Auersch, L., Schmid, G. A simple boundary element formulation and its application to wavefield excited soil-structure interaction. Earthquake Engineering and Structural Dynamics, 19, 931-947 (1990).

[21] Auersch, L. and Rücker, W. Praxisgerechtes Prognosemodell fur Erschutterungen – Einfache Rechenverfahren fur die Emission, Transmission und Immission, *VDI-Berichte 1754 "Baudynamik"*, VDI-Verlag, Dusseldorf, 1-22, (2003).

[22] Auersch, L. Simplified methods for wave propagation and soil-structure interaction: the dispersion of layered soil and the approximation of FEBEM results, Proc. 6th Int. Conf. on Structural Dynamics (Eurodyn 2005), Millpress, Rotterdam, 1303-1309, (2005).

[23] Auersch, L. Ground vibration due to railway traffic – the calculation of the effects of moving static loads and their experimental verification, *Journal of Sound and Vibration*, **293**, 599-610, (2006).

[24] Rosenthal, V., Muller-Boruttau, F. , and Breitsamter, N. How the ballast carries its load - ballast pressure measurements performed on the permanent way SYSTEME GROTZ BSO/MK, World Congress on Railway Research, Cologne, CD-ROM, (2001).

[25] Auersch, L., Baeßler, M., Dietrich, T., and Holzlöhner, U. Dynamik und Setzungen von Bahnfahrwegen auf homogenem und inhomogenem Untergrund, Vorträge der Baugrundtagung 2000 in Hannover, Verlag Glückauf, Essen, 273-282, (2000).

[26] Rucker, W., Auersch, L., Gerstberger, U., and Meinhardt, C. A practical method for the prediction of railway vibration, Proc. 6th Int. Conf. on Structural Dynamics (Eurodyn 2005), Millpress, Rotterdam, 601-606, (2005).

[27] Gerstberger, U. Prediction of dynamic loads beneath tunnels due to railway traffic, Proc. 6th Int. Conf. on Structural Dynamics (Eurodyn 2005), Millpress, Rotterdam, 2053-2058, (2005).